

Sustainable Energy for Water Desalination System Relative to Basra Climate

Amani J. Majeed^{* a}, Ghadeer J. Mohammed^b, Dr. Ala'a Abdulrazaq^c

^a Petroleum Engineering Dept., College of Engineering, Basra University, Iraq.

^b Chemical Engineering Dept., College of Engineering, Basra University, Iraq.

^c Chemical Engineering Dept., College of Engineering, Basra University, Iraq.

Received 17 June 2014

Accepted 22 March 2015

Abstract

The use of solar energy in thermal desalination processes is one of the most promising applications of renewable energy technology. This paper deals with the principle of using solar energy to produce distillate water. The design model contains a solar collector that moves in two dimensions to absorb the direct solar energy, a heat exchanger, two multi-effect distillation units, and a condenser. This model was simulated under Basra weather conditions for four months in 2012. The results showed that the productivity of the proposed desalination system are 5.3, 6.4, 5.3, and 4.4m³/hour for the four months March, June, September and December, respectively. Moreover, inclusion of a thermal fluid heat transfer process, inside the absorber tubes, has improved the productivity of the system.

© 2015 Jordan Journal of Mechanical and Industrial Engineering. All rights reserved

Keywords: Solar energy; Desalination system; Basra weather conditions.

Nomenclature			
A	Heat transfer area (m ²)	h_{od}	Shell side fouling factor (W/m ² .K)
A_{g2}	Outer side cross section area of glass envelope (m ²)	j_h	Heat transfer factor
A_T	Surface area of tube (m ²)	k_f	Thermal conductivity of fluid (W/m.K)
C_{pc}	Heat capacity of cold fluid (kJ/kg.K)	K_t	Constant
C_{ph}	Heat capacity of hot fluid (kJ/kg.K)	k_w	Thermal conductivity of tube wall material (W/m.K)
D_{a2}	Outer side diameter of absorber (m)	L	Tube length (m)
D_b	Bundle diameter (mm)	m_c	Mass flow rate of cold fluid (kg/s)
D_g	Diameter of glass envelope (m)	m_h	Mass flow rate of hot fluid (kg/s)
D_{g1}	Inner side diameter of glass envelope (m)	N_t	Number of tube in tube bundle
D_s	Shell diameter (mm)	n_1	Constant
d_e	Equivalent diameter (mm)	P	Pressure (bar) in Eq.(21 , 26) Pressure (KPa) in Eq.(5)
d_i	Tube inside diameter (mm)	P_C	Critical pressure (bar)
d_o	Tube outside diameter (mm)	P_r	Prandtl number
F	Log mean temperature difference correction factor	P_t	Tube pitch (mm)
G	Gravitational acceleration (m/s ²)	Q_{out}	Thermal loss from collector (kJ/s)
h_i	Heat transfer coefficient inside tube (W/m ² .K)	Re	Reynolds number
h_{id}	Tube side fouling factor (W/m ² .K)	r_{a1}	Inner side radius of absorber (m)
h_o	Heat transfer coefficient outside tube (W/m ² .K)	r_{a2}	outer side radius of absorber (m)
		r_{g1}	Inner side radius of glass envelope (m)

* Corresponding author. e-mail: a_j295@yahoo.com.

r_{g2}	outer side radius of glass envelope (m)
S	Dimensionless temperature ratio
T_{a1}	Inner side temperature of absorber (K)
T_{a2}	Outer side temperature of absorber (K)
$T_{c,in}$	Tube side inlet temperature (K)
$T_{c,out}$	Tube side outlet temperature (K)
T_f	Temperature of heating transfer fluid (K)
T_{g1}	Inner side temperature of glass envelope (K)
T_{g2}	Outer side temperature of glass envelope (K)
$T_{h,in}$	shell side inlet temperature (K)
$T_{h,out}$	shell side outlet temperature (K)
T_{lm}	Logarithmic mean temperature difference
T_m	Mean temperature difference
T_w	Tube wall temperature
T_∞	Temperature evaluation at free stream conditions
$t_{c,in}$	Tube side inlet temperature ($^{\circ}\text{C}$)
$t_{c,out}$	Tube side outlet temperature ($^{\circ}\text{C}$)
$t_{h,in}$	shell side inlet temperature ($^{\circ}\text{C}$)
$t_{h,out}$	shell side outlet temperature ($^{\circ}\text{C}$)
U_o	Overall heat transfer coefficient based on tube outside area ($\text{W}/\text{m}^2\cdot\text{K}$)
u_T	Tube side fluid velocity (m/s)
ε_{g1}	Inner side emissivity of glass envelope
ε_{g2}	outer side emissivity of glass envelope
$\eta_{opt.}$	Optical Efficiency
τ_g	Transmissivity of glass envelope

1. Introduction

Sustainable Energy describes clean sources of energy that has fewer environmental impacts than conventional energy generating technologies. Sustainable sources of energy include solar, wind, hydro, biomass and geothermal. The lack of potable water poses a big problem in the arid regions of the world where freshwater is becoming more scarce and expensive. The availability of clean drinking water is one of the most important international health issues today. The growing world population, together with increased industrial and agricultural activity all over the world, contributes to the depletion and pollution of freshwater resources. Desalination is one of earliest forms of water treatment, still commonly used throughout the world today. Desalination is a process that removes dissolved minerals from seawater and treated wastewater. A number of technologies have been developed for desalination including reverse osmosis (RO), distillation, electro dialysis and vacuum freezing [1]. Distillation is a method

of separating mixtures based on difference in their volatilities in a boiling liquid mixture. The most common method of distillation includes multistage flash (MSF), multi effect distillation (MED) and vapor compression (VC). In MSF, the feed water is heated and the pressure is lowered, so the water “flashes” into steam. In MED, the feed water passes through a number of evaporators in series. Vapor from one series is then condensed and evaporated in the next series to reduce the concentration of impurities [1].

Kalogirou [2] estimated that the production of $1000\text{m}^3/\text{day}$ of freshwater requires 10,000 tons of oil per year. This is a significant as it involves a recurrent energy expense which few of the water-scarce areas of the world can afford. Large commercial desalination plants using fossil fuel are used by a number of oil-rich countries to supplement the traditional sources of water. People in many other countries have neither the money nor the oil resources to allow them to develop in a similar manner. Problems relevant to the use of fossil fuels could be resolved by considering possible utilization of renewable energy resources instead of fossil fuels.

Solar energy has the greatest potential of all the sources of the renewable energy and if a small amount of this form of energy could be used, it will be one of the most important energy supplies, especially when other sources in the country have depleted. Solar power is approximately equal to 1017 kW and the total demand is 1013 W . Therefore, the sun gives 1000 times more power than required. If 5% of this energy can be used, it will be 50 times what the world will require. The energy radiated by the sun on a bright sunny day is $4\text{ to }7\text{ kWh per m}^2$ [3].

Dai and Zang [4-5] proposed an open-air cycle desalination system, in which seawater heated by the sun in a collector and then sprayed on the surface of a honeycomb wall in the humidifier. The air that became hot and humid as it blown through the humidifier led to the condensation area between the feed water tubes, where it cooled and fresh water condensates in the collection container. In order to increase the thermal efficiency, the part of the warm seawater that was not picked up by the air in the honeycomb collected and led back into the seawater tank for another round in the humidification-dehumidification process. Since the air flowed in a straight line, unnecessary pressure losses were avoided. During experiments with this desalination system, a freshwater gain of $6.2\text{ kg}/\text{m}^2$ per day was observed for cases when solar radiation was $700\text{ W}/\text{m}^2$ and the operation time was 8 hours per day. The thermal efficiency of the system was estimated to be 85%.

An interesting study is presented by Chafik [6], where the air is heated and humidified in several steps inside a simple solar collector, This lead to higher vapour content in the air and a lower required airflow rate. Air with an initial temperature and specific humidity of 25°C and $10\text{ g vapour}/\text{kg dry air}$, respectively, enters the solar air-heating collector. During the first step in the collector, the air is warmed to 50°C and then humidified by sprinklers with seawater until the air is approximately saturated. Due to the heat required for the evaporation of the water, the air temperature decreases to about the wet bulb temperature of 23°C . In the next step, the air again heated to 50°C and then humidified in the same way to vapor content of 28 g

vapour/kg dry air. The air temperature goes down to 31°C. During the third step the air is heated to 56°C and humidified to 36 g vapour/kg dry air at 35°C.

2. System Description

As shown in Figure (1) the proposed desalination system consists of a solar collector, a steam generator, a multi-effect distillation unit (MED) and a condenser. The reflective parabolic surface of collector focuses the solar direct radiation on the linear absorber.

The solar radiation is converted to thermal energy, which is absorbed by heat transfer fluid (HTF) flow through the collectors. The water is pumped from the sea through the condenser, where it is heated by energy transferred from the warm steam leaving the evaporator^[7]. The water is then vaporized in the steam generator before it flows into the evaporators (MED) due to the absorption of heat from HTF out of the collectors.

3. Mathematical Modeling

3.1. Solar Collectors Design Equation

In order to design the solar collector system and predict overall system performance, it was necessary to build a mathematical model for the parabolic trough solar collector.

In a steady state, the performance of a parabolic trough solar collector is described by an energy balance that indicates the distribution of incident solar energy into useful energy gain, thermal losses, and optical losses. The solar radiation absorbed by the receiver, \dot{Q}_{abs} , on an hourly basis is equal to the multiply of direct incident solar radiation I_{dn} , the optical efficiency η_{opt} , and the cross sectional area, A_a as shown in Equation(1). The optical efficiency of a collector estimated Equation (2), where A is the effective area ratio [8].

$$\dot{Q}_{abs} = A_a \eta_{opt} I_{dn} \tag{1}$$

$$\eta_{opt} = r \tau_g \alpha A \eta_{op} \tag{2}$$

The thermal loss from the collector to the surroundings is calculated by considerable detail heat transfer Equation here [8].

$$\dot{Q}_{out} = \dot{Q}_{abs} - \dot{Q}_{loss} \tag{3}$$

The solar radiation, calculated by Equation (4), is absorbed by glass envelope and the absorber tube, the energy loss through glass envelope and support structure, calculated by Equation (5), is due to convection and radiation from glass to surrounding and conduction between the absorber and support structure, respectively.

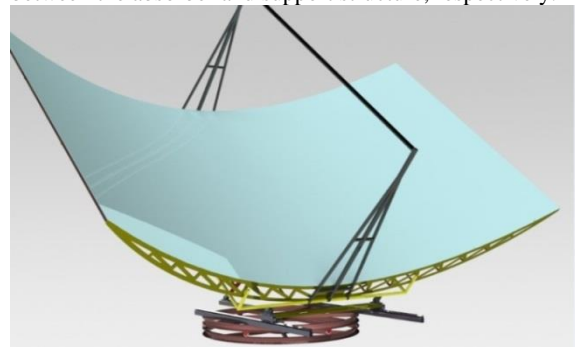


Figure 2. Parabolic Trough Collector with two-axis Tracking Surface

$$\hat{q}_{SolAbs} = q_i \alpha_g K_i + q_i \tau_g \alpha_a K_i \tag{4}$$

$$\hat{q}_{Thermalloss} = \sigma A_{g2} \varepsilon_{g2} \left(T_{g2}^4 - T_{sky}^4 \right) + \pi D_g h(T_g - T_{\psi}) + \sqrt{hPAK} \left(T_{base} - T_{\infty} \right) \tag{5}$$

Where,

$$T_{sky} = 0.0552 T_{\infty}^{1.5} \tag{6}$$

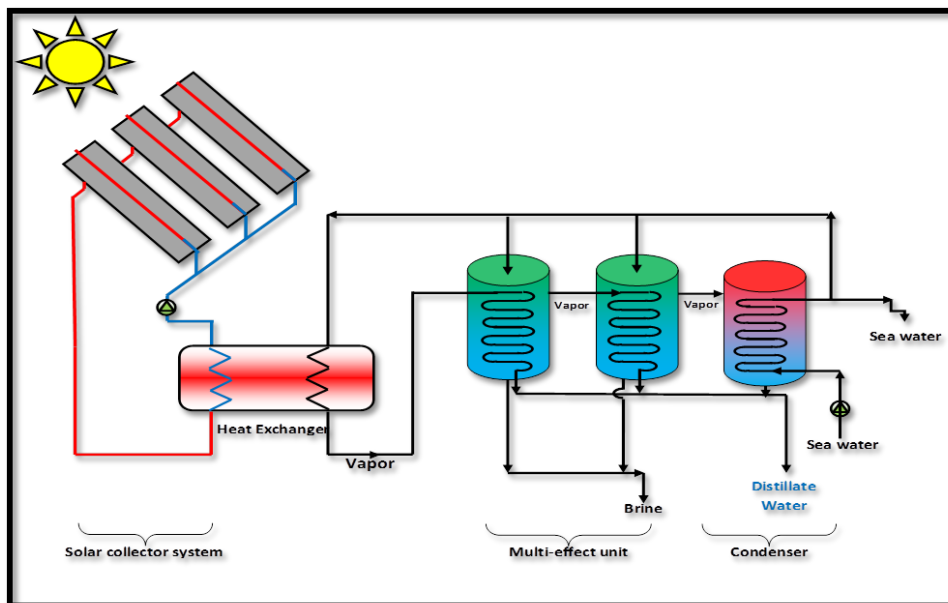


Figure 1. Schematic of the Thermal Solar Distillation system

For the outer surface of the glass, the heat gained from solar radiation (\hat{q}_s) and glass (\hat{q}_g) by conduction is equal to the heat losses from the outer surface to ambient by means of convection (\hat{q}_c) and radiation (\hat{q}_r), indicated in Equation (7).

$$\hat{q}_s + \hat{q}_g = \hat{q}_c + \hat{q}_r \quad (7)$$

Where,

$$\hat{q}_s = q_i \alpha_g K_i \quad (7a)$$

$$\hat{q}_g = \frac{2 \pi k (T_{g1} - T_{g2})}{\ln(r_{g2} / r_{g1})} \quad (7b)$$

$$\hat{q}_c = \pi D_g h (T_{g2} - T_\infty) \quad (7c)$$

$$\hat{q}_r = \sigma A_{g2} \varepsilon_{g2} (T_{g2}^4 - T_{sky}^4) \quad (7d)$$

For the inner surface of glass, heat gained from the absorber outer surface to the inner surface of glass by convection ($\hat{q}_{c,g}$) and radiation ($\hat{q}_{r,g}$). It is equal to the heat loss by means of the conduction through glass as (\hat{q}_g) shown in Equation (8).

$$\hat{q}_g = \hat{q}_{c,g} + \hat{q}_{r,g} \quad (8)$$

Where,

$$\hat{q}_{c,g} = \pi D_{a2} h (T_{a2} - T_{g1}) \quad (8a)$$

$$q_{r,g} = \frac{\sigma \pi D_{a2} (T_{a2}^4 - T_{g1}^4)}{\frac{1}{\varepsilon_{a2}} + \frac{D_{a2}}{D_{g1}} \left(\frac{1}{\varepsilon_{g1}} - 1 \right)} \quad (8b)$$

The heat conducted to absorber is equal to the heat transferred by convection from absorber to the heat transfer fluid shown in Equation (9) [9-14].

$$\hat{q}_{cond-a} = \hat{q}_{conv_fluid} \quad (9)$$

Where;

$$\hat{q}_{cond-a} = \frac{2 \pi k (T_{a1} - T_{a2})}{\ln(r_{a2} / r_{a1})} \quad (9a)$$

$$\hat{q}_{conv_fluid} = \pi D_h h (T_{a1} - T_f) \quad (9b)$$

3.2. Heat Exchangers

Heat exchangers are devices that facilitate the exchange of heat between two fluids at different temperatures while keeping them from mixing with each other. They are commonly used in practices in a wide range of application, from heating in household to chemical processing in large plants [15].

Heat exchangers may be called by other names depending upon their specific purpose. Such as, cooler,

condenser, vaporizer, heater and if two process fluids exchange heat, the term heat exchanger is used [16].

3.2.1. Calculate Heat Duty:

According to the first law of thermodynamics, the heat transfer across a surface involving phase change is given by;

$$Q = m_c C_{pc} (T_{c,out} - T_{c,in}) + m_c \lambda$$

$$= m_h C_{ph} (T_{h,in} - T_{h,out}) + m_h \lambda \quad (10)$$

The rate of heat transfer in a heat exchanger can also be expressed in an analogous manner to Newton's law of cooling as [15]

$$Q = U A \Delta T_m \quad (11)$$

In order to have good results, the following assumptions must be made:

- The heat exchanger is at steady state.
- Each stream has a constant specific heat.
- The overall heat transfer coefficient is constant.
- There are no heat losses from the heat exchanger.
- There is no longitudinal heat transfer in the heat exchanger.
- The flow is counter-current.

3.2.2. Calculate Logarithmic Mean Temperature Difference:

The logarithmic means of the terminal temperature differences [17] is calculated as:

$$\Delta T_{lm} (LMTD) = \frac{(t_{h,in} - t_{c,out}) - (t_{h,out} - t_{c,in})}{\ln \left(\frac{t_{h,in} - t_{c,out}}{t_{h,out} - t_{c,in}} \right)} \quad (12)$$

In design, a correction factor is applied to the ΔT_{lm} to allow for the departure from true countercurrent flow to determine the true temperature difference [18]

$$\Delta T_m = F \Delta T_{lm} \quad (13)$$

The correction factor is a function of the temperature of the fluids and the number of tube and shell passes and is correlated as a function of two dimensionless temperature ratios [17]

$$R = \frac{t_{h,in} - t_{h,out}}{t_{c,out} - t_{c,in}} = \frac{\text{range of shell fluid}}{\text{range of tube fluid}} \quad (14)$$

$$S = \frac{t_{c,out} - t_{c,in}}{t_{h,in} - t_{c,in}} = \frac{\text{range of tube fluid}}{\text{maximum temperature difference}} \quad (15)$$

3.2.3. Choose Shell and Tube Passes

The single shell pass type is by far the most commonly used. The fluid in the tube is usually directed to flow back and forth in a number of "passes" through groups of tubes arranged in parallel, to increase the length of the flow path, In order to give the required tube-side design velocity. Exchangers are built with from one to up to about sixteen tube passes.

3.2.4. Assume an Initial Value for the Overall Heat Transfer Coefficient

There are many typical values for the heat transfer coefficient for a various type of heat exchanger which can be taken as a trail values for starting a thermal design. They are given in Table 1 [19]

3.2.5. Calculate the Total Area of the Heat Exchanger

$$A = \frac{Q}{U \Delta T_m} \quad (16)$$

3.2.6. Choose Diameter and Length of Tubes

Tubes diameters are in the range of 16mm to 50mm. Smaller diameters are preferred because they will give a more compact and therefore cheaper heat exchanger. Larger tubes will be selected for heavily fouling fluids.

The preferred lengths of tubes for heat exchangers are: 1.83 m, 2.44 m, 3.66 m, 4.88 m, 6.10 m and 7.32 m. The use of longer tubes will reduce the shell diameter which will generally result in a lower cost exchanger. The optimum tube length to shell diameter will usually fall within the range of 5 to 10 [19].

3.2.7. Calculate Area of One Tube

$$A_T = \pi d_o L \quad (17)$$

3.2.8. Calculate Number of Tube

$$N_t = A / A_T \quad (18)$$

3.2.9. Select Tube Pitch Arrangement

The tubes in a heat exchanger are usually arranged in an equilateral triangular, square, or rotated square pattern.

- The triangular and rotated square patterns give higher heat-transfer rates and has higher shell side pressure drop.
- A square, or rotated square arrangement, is used for heavily fouling fluids.

$$P_t = 1.25 d_o \quad (19)$$

3.2.10. Calculate Bundle Diameter

The bundle diameter will depend not only on the number of tubes but also on the number of tube passes because spaces must be left in the pattern of tubes on the tube sheet to accommodate the pass partition plates.

$$D_b = d_o \left(\frac{N_t}{K_t} \right)^{1/n_t} \quad (20)$$

The values of N_t and K_t constants are given in Table 2 [19].

3.2.11. Calculate the Shell-Bundle Clearance

The shell diameter must be fit to the tube bundle to reduce bypassing round the outside of the bundle. The typical values of clearance are given in Figure 19 [19]. It will depend on the heat exchanger type.

$$D_s = D_b + \text{clearance} \quad (21)$$

3.2.12. Calculate Tube Side Heat Transfer Coefficient

1. Steam Generator:-

$$h_T = 0.104 (P_C)^{0.69} (q)^{0.7} [1.8 (P / P_C)^{0.17} + 4 (P / P_C)^{1.2} + 10 (P / P_C)^{10}] \quad (22)$$

2. Multi Effect (MED):-

$$h_T = 0.815 \left(\frac{\kappa_L \rho_L (\rho_L - \rho_V) g \lambda}{\pi \mu_L d_o (T_{sat} - T_w)} \right)^{0.25} \quad (23)$$

Where physical properties are at wall temperature

$$T_w = \text{Mean Shell Temperature} + \text{Mean Tube Temperature}$$

3. Condenser:-

$$h_T = 4200 (1.35 + 0.02 t) u_T^{0.8} / d_o^{0.2} \quad (24)$$

3.2.13. Calculate Shell-side Heat Transfer Coefficient

1. Steam Generator:-

$$h_s = (\kappa_f / d_e) j_h Re Pr^{1/3} \quad (25)$$

Where physical properties are at mean shell temperature and

$$d_e = (1.10 / d_o) (P_t^2 - 0.917 d_o^2) \quad (26)$$

2. Multi Effect (MED):-

$$h_s = 0.104 (P_C)^{0.69} (q)^{0.7} [1.8 (P / P_C)^{0.17} + 4 (P / P_C)^{1.2} + 10 (P / P_C)^{10}] \quad (27)$$

3. Condenser:-

$$h_T = 0.725 \left(\frac{\kappa_L^3 \rho_L (\rho_L - \rho_V) g \lambda}{\mu_L d_o (T_{sat} - T_w)} \right)^{0.25} \quad (28)$$

Where physical properties are at wall temperature

3.2.14. Select Fouling Factors

Most fluids will foul the heat-transfer surfaces in an exchanger duo to the deposition of material which have a relatively low thermal conductivity and will reduce the overall heat transfer coefficient. The effect of fouling is allowed for in design by including the inside and outside fouling coefficients, Table 3 [19].

Fouling factor for seawater is $2000 \text{ W/m}^2 \cdot \text{C}$

Fouling factor for water is $4000 \text{ W/m}^2 \cdot \text{C}$

Fouling factor for HTF is $\text{W/m}^2 \cdot \text{C}$

3.2.15. Calculate the Overall Heat Transfer Coefficient:-

$$\left(\frac{1}{U_o} = \frac{1}{h_o} + \frac{1}{h_{od}} + \frac{d_o \ln(d_o/d_i)}{2k_w} + (d_o/d_i) \left(\frac{1}{h_{id}} + \frac{1}{h_i} \right) \right) \quad (29)$$

4. Results and Discussion

Figures from (3) to (6) show that the absorbed solar energy (that absorbed by glass envelope and absorber tube) vs. time for a specified day 15th of each month in 2012, demonstrated that the value of solar energy that absorbed by absorber tube is larger than that absorbed by the glass envelope, this is acceptable because the absorbed energy depend on the absorptivity and the type of the absorber; therefore, when the absorber tube surface supported with selective coating, the tube absorbs large amount of energy because of the two dimensions parabolic through collector, the collector absorbed large amount of solar energy.

Figures from (7) to (10) explain the related collector outlet temperature (that out from solar collector) vs. time, and the temperature of heat transfer fluid that leave the heat exchanger which calculated through simulation with the discussed plant model for a specified day 15th of (March, June, September, and December) in 2012.

Figures (11) to (14) Show the effect of time on the value of the overall heat transfer coefficient in four different months. It is clear that the value of the overall heat transfer coefficient is increasing with time until 12 PM because with time temperature of HTF will be increased, and that because the amount of heat absorbed by the absorber tube glass will be increased until 12 PM. After 12 PM, temperature of HTF will be decreased with time and that because the amount of heat absorbed by the absorber tube glass will be decreased with time. The value of the overall heat transfer coefficient will be increased with time until 12 PM due to the increasing in the amount of heat absorbing by the tube glass and vs. versa.

Figures (15) to (17) Show the effect of time on the production of distilled water. These figures show that the production of distilled water will be increased with time, since the amount of steam produced from steam generator per hour is constant. So the water distillate per hour will be constant and the accumulative amount of distilled water will be increase with time.

The same figures Show the effect of time on the overall production of distilled water. These figures show that the production of distilled water will be increased with time, since the rate of steam produced from each effect which will inter the next effect is constant. So the rate of water distillate will be constant and the accumulative amount of distilled water will be increase with time.

Figure (18) shows that the large production of distilled water was been at June. This is because the hot weather of Basra and the long day hours at June, which means the amount of heat absorbed by the absorber tube glass will be larger than that at March, September and December.

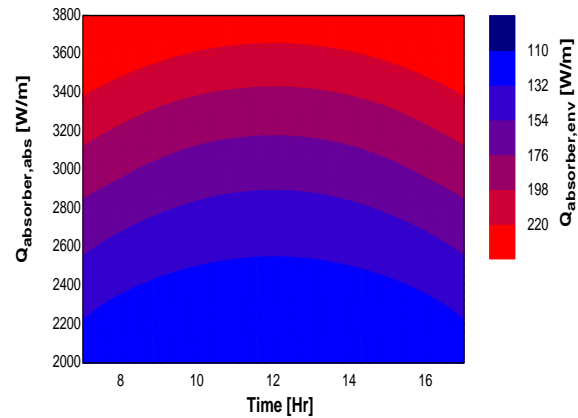


Figure 3. Absorbed Solar Energy from Collector by Absorber Tube & Glass Envelope for 15 March 2012.

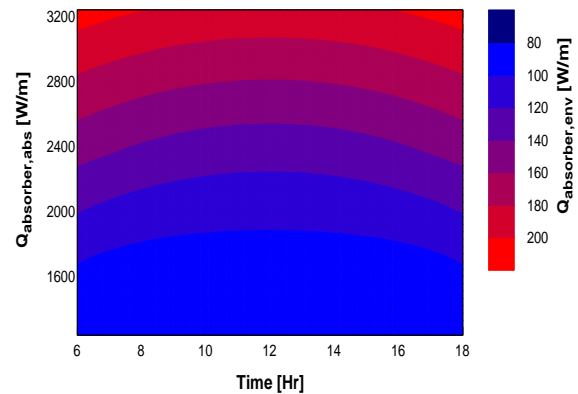


Figure 4. Absorbed Solar Energy from Collector by Absorber Tube & Glass Envelope for 15 June 2012.

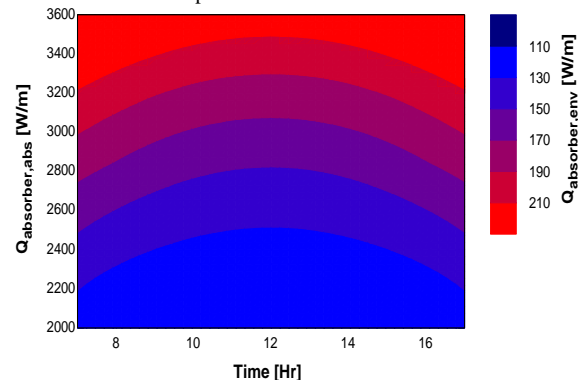


Figure 5. Absorbed Solar Energy from Collector by Absorber Tube & Glass Envelope for 15 September 2012.

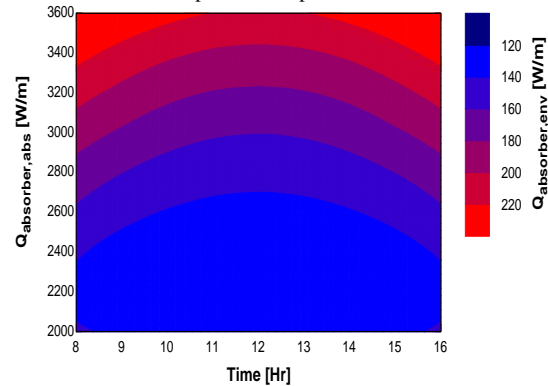


Figure 6. Absorbed Solar Energy from Collector by Absorber Tube & Glass Envelope for 15 December 2012.

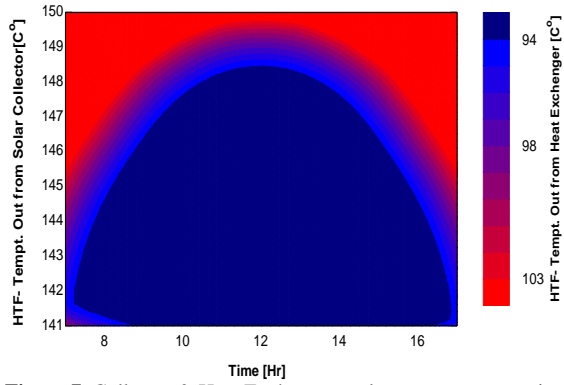


Figure 7. Collector & Heat Exchanger outlet temperature vs. time on 15 May 2012

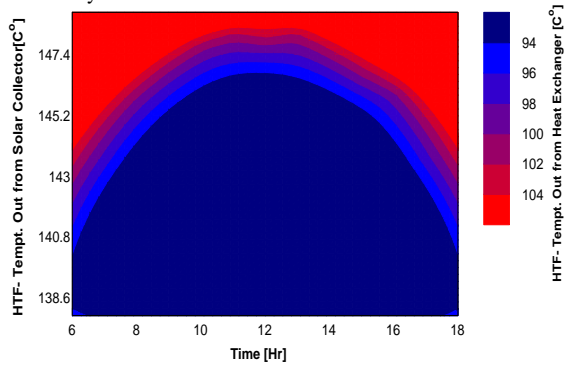


Figure 8. Collector & Heat Exchanger outlet temperature vs. time on 15 June 2012

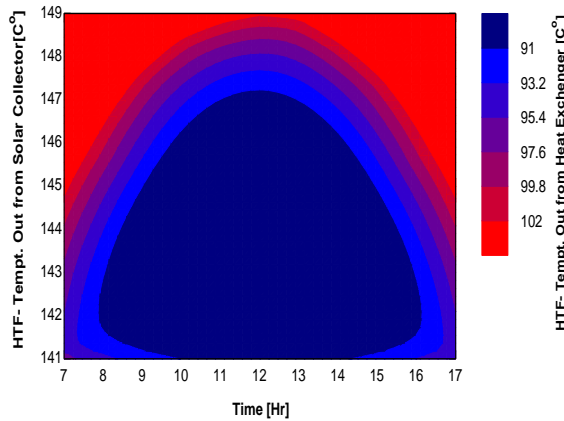


Figure 9. Collector & Heat Exchanger outlet temperature vs. time on 15 September 2012

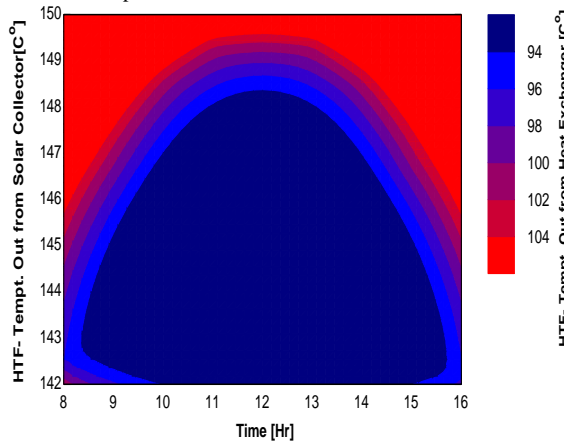


Figure 10. Collector & Heat Exchanger outlet temperature vs. time on 15 December 2012

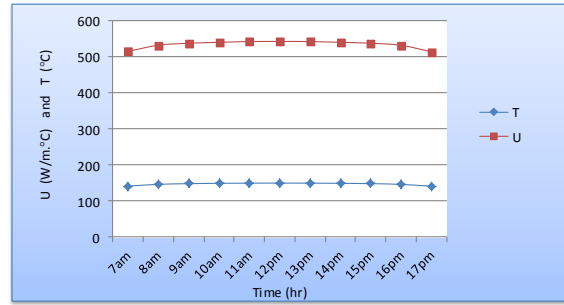


Figure 11. Shows the change in the values of temperature and overall heat transfer coefficient vs. time on March in the first effect.

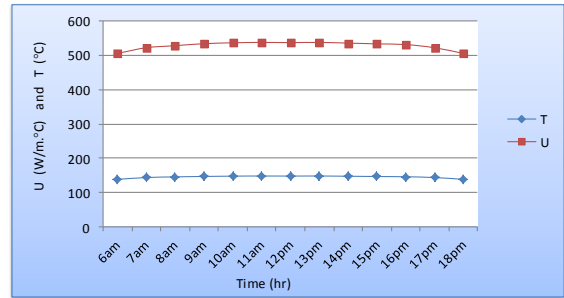


Figure 12. Shows the change in the values of temperature and overall heat transfer coefficient vs. time on June in the first effect.

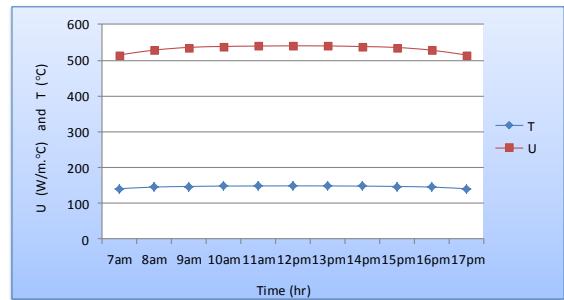


Figure 13. Shows the change in the values of temperature and overall heat transfer coefficient vs. time on September in the first effect.

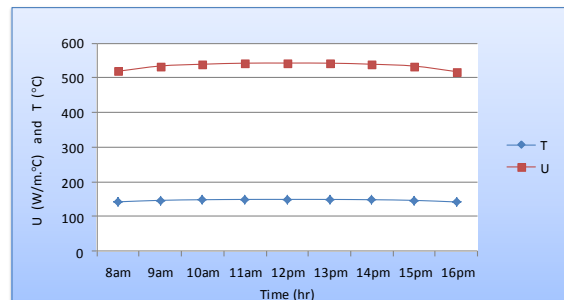


Figure 14. Shows the change in the values of temperature and overall heat transfer coefficient vs. time on November in the first effect.

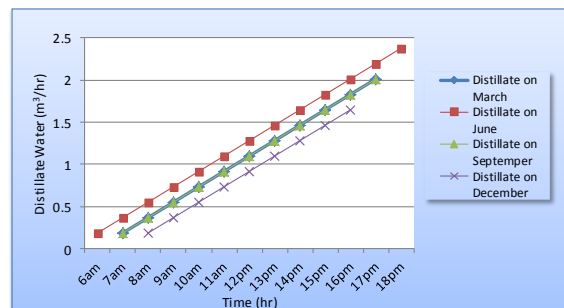


Figure 15. Shows the amount of water produce from first effect during four month.

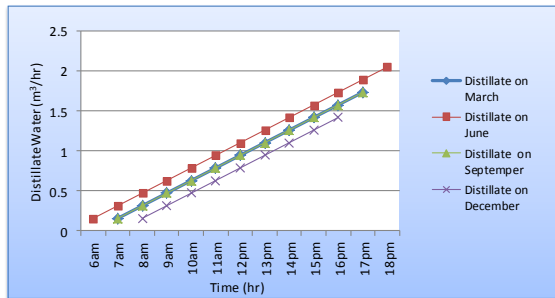


Figure 16. Shows the amount of water produce from second effect during four month.

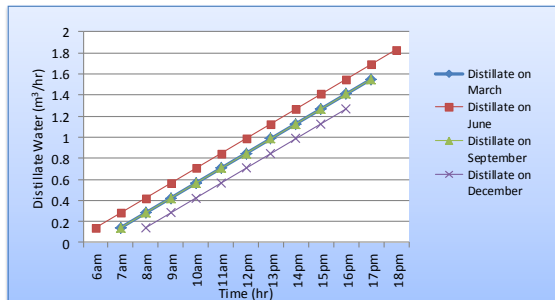


Figure 17. Shows the amount of water produce from condenser during four month.

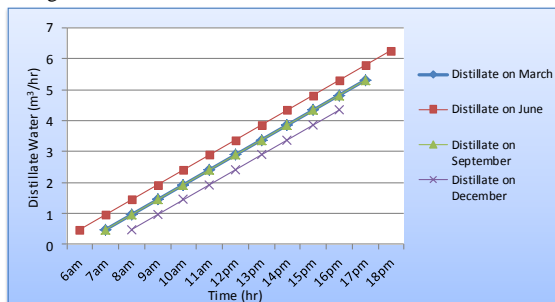


Figure 18. Shows the amount of water produce from the plant during four month.

5. conclusion

- The ability of using the solar system in the regions suffering from water scarcity. The nature of weather in Basra city support the ability of using the solar system with acceptable rate of production especially during the crises or emergency times.
- The record values of Basra climate conditions (solar intensity and outlet temperature of collector) for four months have shown a high fluctuation from month to month. So the water productivity varied between (4.4 - 6.4) m³/hr.
- The relation between water productivity and solar intensity is proportional.

References

[1] F.A. Oyawale, A.O. Odior, M.M. Ismaila, "Design and Fabrication of a Water Distiller". Journal of Emerging Trends

in Engineering and Applied Sciences, Vol. 1 (2010) No. 2, 168-173.

[2] S.A. Kalogirou, "Seawater desalination using renewable energy sources". Progress in Energy and Combustion Science, Vol. 31 (2005) No. 3, 242-281.

[3] A. Kumar, G.D. Sootha, P. Chaturvadi, "Performance of a multi-stage distillation system using a flat-plate collector". Extended Abstract, ISES Solar World Congress, Kobe, Japan, (1989).

[4] Y.J. Dai, R.Z. Wang, H.F. Zhang, "Parametric analysis to improve the performance of a solar desalination unit with humidification and dehumidification". Desalination, Vol. 142 (2002) No. 2, 107-118.

[5] Y.J. Dai, H.F. Zhang, "Experimental investigation of a solar desalination unit with humidification and dehumidification". Desalination, Vol. 130 (2000) No. 2, 169-175.

[6] E. Chafik, "A new seawater desalination process using solar energy". Desalination, Vol. 153 (2003) No. 1-3, 25-37.

[7] C. Lourens, E. Uken, M. Kilfoil, "Low Temperature Solar Powered Distillation of Seawater". Cape Peninsula University of Technology, Cape, South Africa, 2006.

[8] N. Mukund, V. Muthu Raman, "Improved Method of Desalination of Seawater with Electric Power Generation using Solar Energy" 2nd International Conference on Environmental Science and Development, Singapore, 2011.

[9] M. Khoukhi, S. Maruyama, "Theoretical approach of a flat plate solar collector with clear and low-iron glass covers taking into account the spectral absorption and emission within glass covers layer". Renewable Energy, Vol. 30 (2005) No. 8, 1177-1194.

[10] R. Forristall, "Heat Transfer Analysis and Modeling of a Parabolic Trough Solar Receiver Implemented in Engineering Equation Solver", National Renewable Energy Laboratory, (2003).

[11] M. Yaghoubi, F. Ahmadi, M. Bandehee, "Analysis of Heat Losses of Absorber Tubes of Parabolic through Collector of Shiraz (Iran) Solar Power Plant" Journal of Clean Energy Technologies, Vol. 1 (2013) No. 1, 33-37.

[12] WIRZ M. Optical and Thermal Modeling of Parabolic Through Concentrator Systems. Dissertation thesis, Bern, (2014).

[13] M. Yaghoubi, K. Azizian, A. Kenary, "Simulation of Shiraz solar power plant for optimal assessment". Renewable Energy, Vol. 28 (2003) No. 12, 1985-1998.

[14] Duffie JA., Beckman WA. Solar Engineering of Thermal Processes. 3rd ed. New York: John Wiley and Sons; 1991.

[15] Cengel Y., Cimbala J., Turner R. Fundamentals of Thermal-Fluid sciences. 4th ed. New York: McGraw-Hill; 2012.

[16] Couper JR., Penney WR., Fair JR. Chemical Process Equipment. 3rd ed. United Kingdom: Butterworth-Heinemann; 2012.

[17] Modi J. Quick Manual Design of Shell and Tube Heat Exchanger. M.Sc. Thesis, Poona University, India, 1991.

[18] Edwards J.E., "Design and Rating Shell and Tube Heat Exchangers", Process and Engineering Services to Industry Worldwide.

[19] Sinnott R.K. Coulson and Richardson's Chemical Engineering series. Volume 6. 3rd ed. United Kingdom: Butterworth-Heinemann; 1991.

Appendix

Table 1. Typical overall coefficients [19],

Shell and tube exchangers		
Hot fluid	Cold fluid	<i>U</i> (W/m ² °C)
<i>Heat exchangers</i>		
Water	Water	800–1500
Organic solvents	Organic solvents	100–300
Light oils	Light oils	100–400
Heavy oils	Heavy oils	50–300
Gases	Gases	10–50
<i>Coolers</i>		
Organic solvents	Water	250–750
Light oils	Water	350–900
Heavy oils	Water	60–300
Gases	Water	20–300
Organic solvents	Brine	150–500
Water	Brine	600–1200
Gases	Brine	15–250
<i>Heaters</i>		
Steam	Water	1500–4000
Steam	Organic solvents	500–1000
Steam	Light oils	300–900
Steam	Heavy oils	60–450
Steam	Gases	30–300
Dowtherm	Heavy oils	50–300
Dowtherm	Gases	20–200
Flue gases	Steam	30–100
Flue	Hydrocarbon vapours	30–100
<i>Condensers</i>		
Aqueous vapours	Water	1000–1500
Organic vapours	Water	700–1000
Organics (some non-condensables)	Water	500–700
Vacuum condensers	Water	200–500
<i>Vaporisers</i>		
Steam	Aqueous solutions	1000–1500
Steam	Light organics	900–1200
Steam	Heavy organics	600–900

Table 2. Fouling factors (coefficients), typical values [19].

Fluid	Coefficient (W/m ² °C)	Factor (resistance) (m ² °C/W)
River water	3000–12,000	0.0003–0.0001
Sea water	1000–3000	0.001–0.0003
Cooling water (towers)	3000–6000	0.0003–0.00017
Towns water (soft)	3000–5000	0.0003–0.0002
Towns water (hard)	1000–2000	0.001–0.0005
Steam condensate	1500–5000	0.00067–0.0002
Steam (oil free)	4000–10,000	0.0025–0.0001
Steam (oil traces)	2000–5000	0.0005–0.0002
Refrigerated brine	3000–5000	0.0003–0.0002
Air and industrial gases	5000–10,000	0.0002–0.0001
Flue gases	2000–5000	0.0005–0.0002
Organic vapours	5000	0.0002
Organic liquids	5000	0.0002
Light hydrocarbons	5000	0.0002
Heavy hydrocarbons	2000	0.0005
Boiling organics	2500	0.0004
Condensing organics	5000	0.0002
Heat transfer fluids	5000	0.0002
Aqueous salt solutions	3000–5000	0.0003–0.0002

Table 3. Constants for use in equation 20 [19].

Triangular pitch, $p_t = 1.25d_o$					
No. passes	1	2	4	6	8
K_1	0.319	0.249	0.175	0.0743	0.0365
n_1	2.142	2.207	2.285	2.499	2.675
Square pitch, $p_t = 1.25d_o$					
No. passes	1	2	4	6	8
K_1	0.215	0.156	0.158	0.0402	0.0331
n_1	2.207	2.291	2.263	2.617	2.643

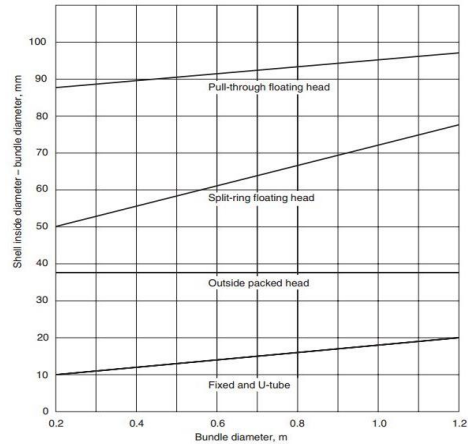


Figure 19. Shell-bundle clearance